M&C 2017 - International Conference on Mathematics & Computational Methods Applied to Nuclear Science & Engineering, Jeju, Korea, April 16-20, 2017, on USB (2017)

An Activation Calculation in a Deep Penetration Problem with AETIUS: An Easy Modeling Discrete Ordinates Transport Code UsIng Unstructured Tetrahedral Mesh, Shared Memory Parallel

Jong Woon KIM[1*] and Young-Ouk LEE[1]

[1]*Korea Atomic Energy Research Institute, 989 Daeduck-daero, Yuseong-gu, Daejeon 305-353, Korea,* [*]*jwkim@kaeri.re.kr*

Abstract - *We describe a brief overview of in-house code, AETIUS, and provide numerical results from both AETIUS and Monte Carlo code, MCNP, in an activation calculation in a deep penetration problem with a small activation volume.*

I. INTRODUCTION

As computing power and parallel processing capabilities are getting better, users prefer to use a method that has less approximation such as a Monte Carlo method.

Of course, the Monte Carlo method is very powerful in various particle transport problems. However, it also has inherent drawbacks in terms of statistics. To achieve better statistics, a lot of people have been developing several variance reduction techniques.

There is another method called a deterministic method. This method requires a discretization of the space, angle, and energy. However, it does not have any statistical issues.

In this paper, we describe a brief overview of in-house code, AETIUS, and provide numerical results from both AETIUS and the Monte Carlo code, MCNP [1], in an activation calculation for a deep penetration problem with a small activation volume.

II. DESCRIPTION OF THE ACTUAL WORK

1. AETIUS (An Easy modeling Transport code usIng Unstructured tetrahedral mesh, Shared memory parallel) code

AETIUS is an in-house transport solver which uses discrete ordinates method, discontinuous finite element S_N method [2], programed using f90, and uses Gmsh [3] as a pre- and post- processing program. A white boundary condition on an arbitrary surface [4], the first collision source method on a point or volume source, and shared memory parallel capabilities [5] have been implemented to the AETIUS. In addition to the discontinuous finite element S_N method, two subcell balance methods [6] had been developed for dealing with an unstructured tetrahedral mesh. But in AETIUS, this method is not implemented yet.

Compared to the other deterministic codes, which use a regular mesh, one of the merits of AETIUS is its capability to deal with a complicated geometry by using unstructured tetrahedral mesh like ATTILA [7]. With a help of CAD tools (e.g., CATIA) and Gmsh, we can finish complicated geometry modeling for AETIUS very easily. Fig. 1 shows the overall calculation flow of AETIUS.

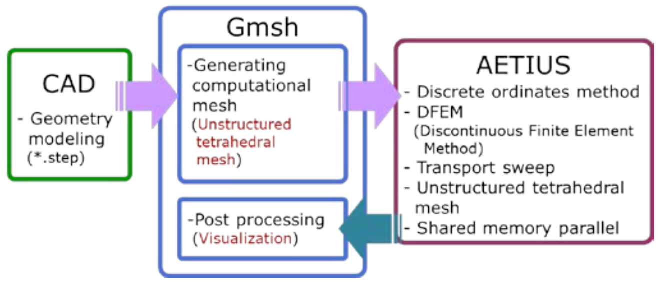

Fig. 1. The overall calculation flow of AETIUS.

2. Transport Calculations

To see the effectiveness and efficiency of AETIUS, we choose an activation calculation in a deep penetration problem with a small activation volume, as shown in Fig. 2.

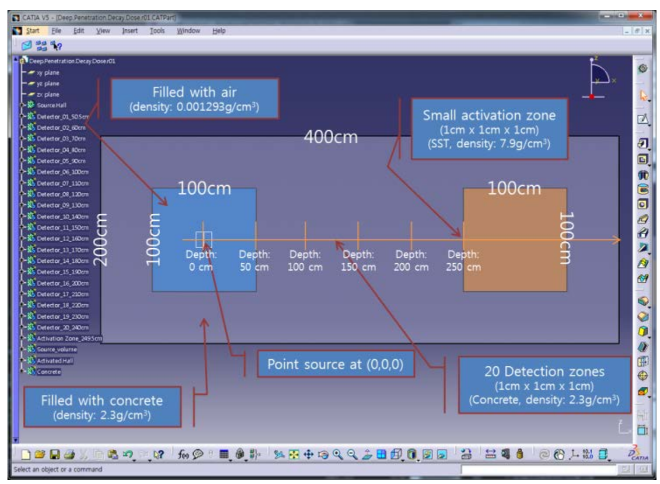

Fig. 2. Overview of an activation calculation in a deep penetration problem with a small activation volume.

Two cubes are located two meters apart from each other. One is at the center of origin (0,0,0) and the other is at (300cm,0,0). Both cubes are filled with air. Concrete covers the outside of the cubes, as shown in Fig. 2.

An imported step file in Gmsh is shown in Fig. 3. The point source is at the origin (0,0,0) and the small activation zone (1cm^3) is at 249.5cm on the x-axis.

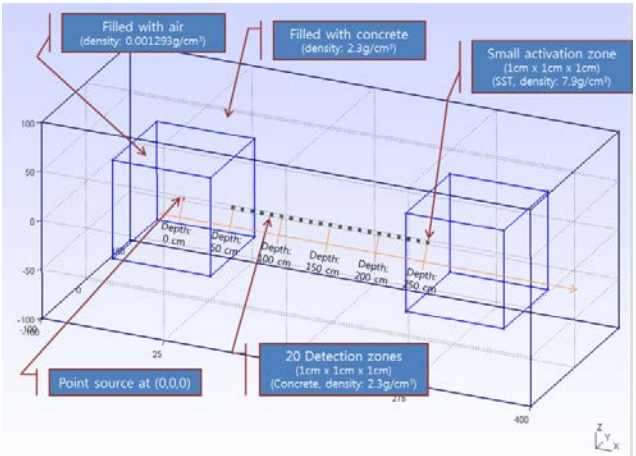

Fig. 3. Imported step file in Gmsh for AETIUS.

Along the x-axis, 20 detection zones (1cm × 1cm ×1cm) are located from 50cm to 240cm. We like to have a neutron spectrum on the small activation zone and use it for an activation calculation. The computational mesh is generated by Gmsh and shown in Fig. 4.

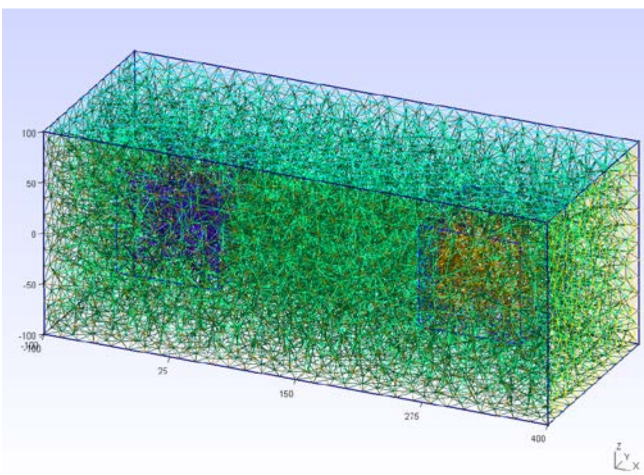

Fig. 4. The computational mesh (generated by Gmsh, 68,206 unstructured tetrahedrons).

In MCNP calculation, to obtain a satisfactory solution in view of statistics, concrete block is divided into multi-slabs to apply weight windows as shown in Fig. 5. Twenty detection zones are filled with concrete but small activation zone is filled with SST (Stainless Steel).

Transport calculations are performed in a deep penetration problem with a small activation volume. This problem seems very simple and easy. However, in view of a Monte Carlo transport code, it may be simple but not easy to obtain solutions with a reliable confidence interval (the relative error is less than 0.1 for all other tallies) [1].

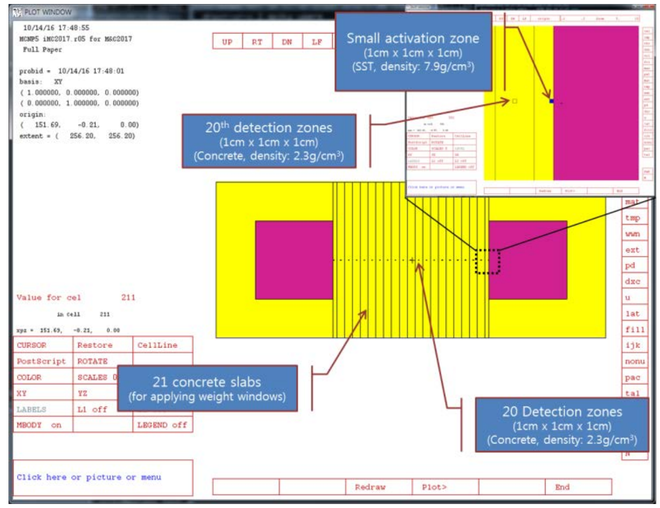

Fig. 5. The geometry modeling for MCNP calculation.

It is hard to send particles deep into the concrete block and the tally zones (detection and activation zones) are small ($1cm^3$). In addition, for an activation calculation, we need a neutron spectrum in the activation zone with a reliable confidence interval. Even though, we might obtain a cell averaged flux tally in the activation zone, the statistics in the neutron spectrum might be poor.

The calculation parameters that are used in transport calculations are listed in Table I.

Table I. Parameters for transport calculations

	MCNP5	AETIUS
Source strength	Point source: 1 source particle at origin (0,0,0)	
Source spectrum	Source is given in the 1st group of VITAMIN-J 175 group structure	
Library	ENDF-B/VII.0	
Energy group structure	Continuous energy	VITAMIN-J (175 Group)
Material density	Air : 0.001293 g/cm^3 Concrete : 2.3 g/cm^3 Stainless Steel : 7.9 g/cm^3	
Order of scattering anisotropy	n/a	3
S_N order	n/a	Triangular Chebyshev-Legendre S_{16}
Number of tetrahedral element	n/a	68,206
Calc. options	F4 tally with weight window	†FCS with point source
Error criterion	nps :1×10^{10}	1×10^{-4}
Parallel	MPI (121 cores)	OpenMP (120 cores)
Elapsed wall clock time	n/a	7.92 hour

†FCS : first collision source method

The calculated total neutron flux from AETIUS is visualized through the Gmsh and shown in Fig. 6.

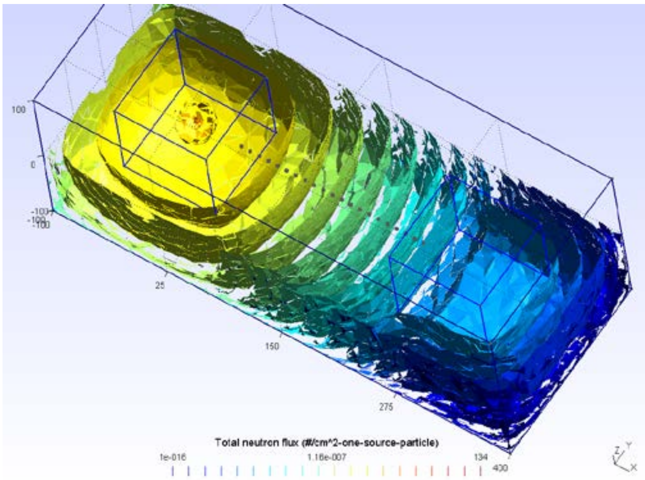

Fig. 6. Visualized total neutron flux isosurface distribution (sectional view of the lower part).

One of the key advantages of using a discrete ordinates code such as AETIUS is that we can obtain solutions throughout the problem in a single run. This is very useful to understand how the flux changes throughout the modeled geometry

Volume averaged fluxes in 21 zones (20 detection zones and one activation zone) are compared with those of MCNP5, and are shown in Fig. 7. These fluxes of AETIUS were obtained through a single run. However, for MCNP5, we have to run it several times to obtain weight windows and re-run it again to send particles to the small activation zone until we have reliable tally results.

The results of the last three tally zones looks well match with those of AETIUS. However, in view of the relative error shown in Fig. 8, they are out of the reliable confidence interval. In the MCNP manual, reliable confidence interval of relative error should be less than 0.1 for all other tallies.

For an activation calculation, neutron spectra of the activation zone from AETIUS and MCNP5 are compared and are shown in Fig. 9.

It seems that the averaged total neutron flux on the activation zone shows similar result compared to the AETIUS result in Fig. 7. However, tallied spectrum of MCNP5 in that zone is poor. Except for the lowest energy group, all other relative errors of other energy groups are 1.0 in this calculation as shown in Fig. 9 and Table II.

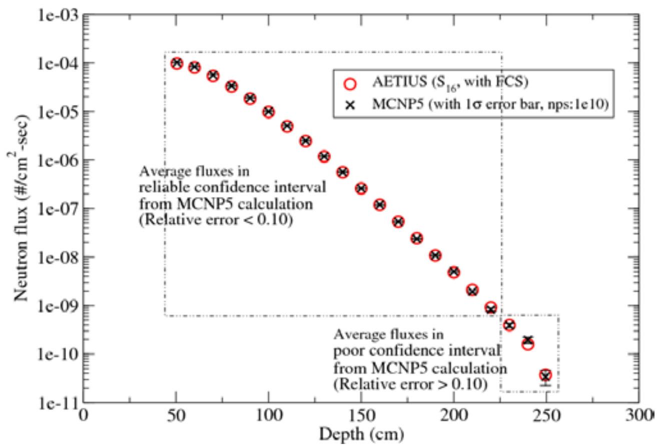

Fig. 7. Comparison of volume averaged fluxes on 20 detection zones and one activation zone.

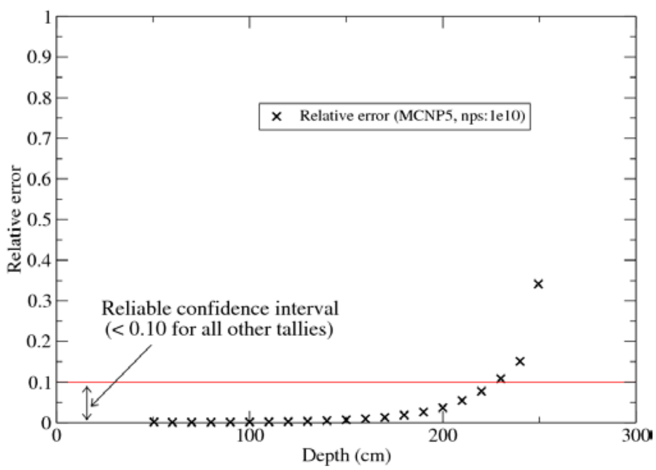

Fig. 8. Relative error of MCNP5 on 21 tally zones.

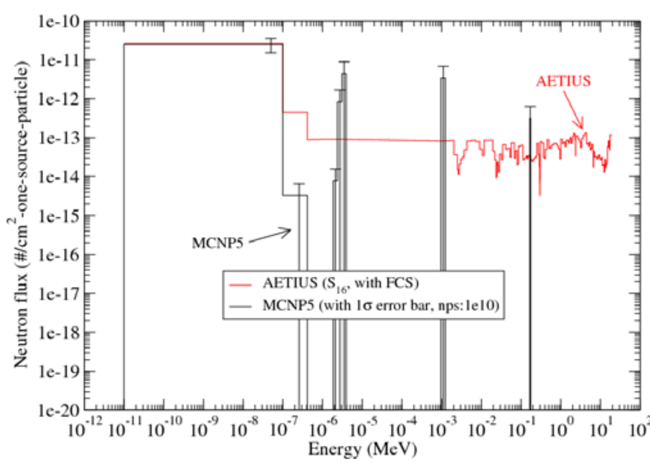

Fig. 9. Comparison of two neutron spectra in the activation zone (175 groups).

For example, if tallied value is X and relative error is R in the MCNP result, then the range of one standard deviation can be calculated as Eq. (1).

$$\text{Range of one standard deviation: } X \pm X \times R. \qquad (1)$$

If relative error, R, is 1.0, then it means that tallied value, X, is 100% error and tallied value cannot be believed reliable.

For easy understanding, the raw data of Fig. 9 is listed in the Table II. In the most energy bins, MCNP5 could not provide particle flux. Even though it does, the relative error is 1.0. More neutrons should be sent to the small activation zone through the thick concrete wall. However, AETIUS provides particle flux through all energy bins since it is deterministic transport solver.

Table II. Two neutron spectra in the activation zone

	MCNP5†		AETIUS
Energy (MeV)	Particle flux (#/cm^2-one-source-particle)	Relative error	Particle flux (#/cm^2-one-source-particle)
1.0000E-11	0.00000E+00	0.0000	0.00000E+00
1.0000E-07	2.50560E-11	0.3904	2.66788E-11
4.1399E-07	3.26885E-15	1.0000	4.43264E-13
5.3158E-07	0.00000E+00	0.0000	8.97910E-14
6.8256E-07	0.00000E+00	0.0000	9.03501E-14
8.7642E-07	0.00000E+00	0.0000	9.07420E-14
1.1254E-06	0.00000E+00	0.0000	9.10114E-14
1.4450E-06	0.00000E+00	0.0000	9.11109E-14
1.8554E-06	0.00000E+00	0.0000	9.11473E-14
2.3824E-06	7.86871E-15	1.0000	9.11002E-14
3.0590E-06	8.30195E-13	1.0000	9.09687E-14
3.9279E-06	4.48528E-12	1.0000	9.08053E-14
5.0435E-06	0.00000E+00	0.0000	9.05742E-14
6.4760E-06	0.00000E+00	0.0000	9.03148E-14
8.3153E-06	0.00000E+00	0.0000	9.00188E-14
1.0677E-05	0.00000E+00	0.0000	8.97004E-14
1.3710E-05	0.00000E+00	0.0000	8.93722E-14
1.7603E-05	0.00000E+00	0.0000	8.89796E-14
2.2603E-05	0.00000E+00	0.0000	8.86296E-14
2.9023E-05	0.00000E+00	0.0000	8.82400E-14
3.7267E-05	0.00000E+00	0.0000	8.78479E-14
4.7851E-05	0.00000E+00	0.0000	8.74312E-14
6.1442E-05	0.00000E+00	0.0000	8.70270E-14
7.8893E-05	0.00000E+00	0.0000	8.66108E-14
1.0130E-04	0.00000E+00	0.0000	8.61919E-14
1.3007E-04	0.00000E+00	0.0000	8.57684E-14
1.6702E-04	0.00000E+00	0.0000	8.53646E-14
2.1445E-04	0.00000E+00	0.0000	8.49169E-14
2.7536E-04	0.00000E+00	0.0000	8.45088E-14
3.5358E-04	0.00000E+00	0.0000	8.41025E-14
4.5400E-04	0.00000E+00	0.0000	8.36794E-14
5.8295E-04	0.00000E+00	0.0000	8.32925E-14
7.4852E-04	0.00000E+00	0.0000	8.29286E-14
9.6112E-04	0.00000E+00	0.0000	8.26599E-14
1.2341E-03	3.40384E-12	1.0000	8.20938E-14
1.5846E-03	0.00000E+00	0.0000	8.31467E-14
2.0347E-03	0.00000E+00	0.0000	8.55008E-14
2.2487E-03	0.00000E+00	0.0000	3.59535E-14
2.4852E-03	0.00000E+00	0.0000	3.61491E-14
2.6126E-03	0.00000E+00	0.0000	1.52202E-14
2.7465E-03	0.00000E+00	0.0000	1.14600E-14
3.0354E-03	0.00000E+00	0.0000	2.06805E-14
3.3546E-03	0.00000E+00	0.0000	2.84507E-14
3.7074E-03	0.00000E+00	0.0000	3.20395E-14
4.3074E-03	0.00000E+00	0.0000	4.82425E-14
5.5308E-03	0.00000E+00	0.0000	8.20581E-14
7.1017E-03	0.00000E+00	0.0000	8.62685E-14
9.1188E-03	0.00000E+00	0.0000	8.00488E-14
1.0595E-02	0.00000E+00	0.0000	5.07934E-14
1.1709E-02	0.00000E+00	0.0000	3.44654E-14
1.5034E-02	0.00000E+00	0.0000	8.69758E-14
1.9305E-02	0.00000E+00	0.0000	8.70204E-14
2.1875E-02	0.00000E+00	0.0000	4.48553E-14
2.3579E-02	0.00000E+00	0.0000	2.72258E-14
2.4176E-02	0.00000E+00	0.0000	9.28331E-15
2.4788E-02	0.00000E+00	0.0000	9.82111E-15
2.6058E-02	0.00000E+00	0.0000	2.39288E-14
2.7000E-02	0.00000E+00	0.0000	1.96503E-14
2.8500E-02	0.00000E+00	0.0000	1.30964E-14
3.1828E-02	0.00000E+00	0.0000	3.77036E-14
3.4307E-02	0.00000E+00	0.0000	2.71855E-14
4.0868E-02	0.00000E+00	0.0000	6.59164E-14
4.6309E-02	0.00000E+00	0.0000	5.02381E-14
5.2475E-02	0.00000E+00	0.0000	5.35063E-14
5.6562E-02	0.00000E+00	0.0000	3.15182E-14
6.7379E-02	0.00000E+00	0.0000	7.39942E-14
7.2000E-02	0.00000E+00	0.0000	2.99484E-14
7.9500E-02	0.00000E+00	0.0000	4.63119E-14
8.2500E-02	0.00000E+00	0.0000	1.97028E-14
8.6517E-02	0.00000E+00	0.0000	2.10073E-14
9.8037E-02	0.00000E+00	0.0000	6.00637E-14
1.1109E-01	0.00000E+00	0.0000	6.37837E-14
1.1679E-01	0.00000E+00	0.0000	2.69187E-14
1.2277E-01	0.00000E+00	0.0000	2.73042E-14
1.2907E-01	0.00000E+00	0.0000	3.00638E-14
1.3569E-01	0.00000E+00	0.0000	3.06875E-14
1.4264E-01	0.00000E+00	0.0000	3.42358E-14
1.4996E-01	0.00000E+00	0.0000	2.90573E-14
1.5764E-01	0.00000E+00	0.0000	3.32958E-14
1.6573E-01	0.00000E+00	0.0000	3.46414E-14
1.7422E-01	3.16177E-13	1.0000	3.25393E-14
1.8316E-01	0.00000E+00	0.0000	2.79934E-14
1.9255E-01	0.00000E+00	0.0000	2.58420E-14
2.0242E-01	0.00000E+00	0.0000	2.49534E-14
2.1280E-01	0.00000E+00	0.0000	2.73039E-14
2.2371E-01	0.00000E+00	0.0000	2.97201E-14
2.3518E-01	0.00000E+00	0.0000	3.13900E-14
2.4724E-01	0.00000E+00	0.0000	3.25639E-14
2.7324E-01	0.00000E+00	0.0000	7.10481E-14
2.8725E-01	0.00000E+00	0.0000	3.67732E-14
2.9452E-01	0.00000E+00	0.0000	1.81989E-14
2.9720E-01	0.00000E+00	0.0000	6.76566E-15
2.9850E-01	0.00000E+00	0.0000	3.28833E-15
3.0197E-01	0.00000E+00	0.0000	8.63322E-15
3.3373E-01	0.00000E+00	0.0000	7.90644E-14
3.6883E-01	0.00000E+00	0.0000	7.30429E-14
3.8774E-01	0.00000E+00	0.0000	3.16906E-14
4.0762E-01	0.00000E+00	0.0000	2.92721E-14
4.5049E-01	0.00000E+00	0.0000	5.01493E-14
4.9787E-01	0.00000E+00	0.0000	8.86563E-14
5.2340E-01	0.00000E+00	0.0000	5.36402E-14
5.5023E-01	0.00000E+00	0.0000	5.66524E-14
5.7844E-01	0.00000E+00	0.0000	5.45593E-14
6.0810E-01	0.00000E+00	0.0000	6.29682E-14
6.3928E-01	0.00000E+00	0.0000	6.53082E-14
6.7206E-01	0.00000E+00	0.0000	6.74735E-14
7.0651E-01	0.00000E+00	0.0000	7.03881E-14
7.4274E-01	0.00000E+00	0.0000	7.05577E-14
7.8082E-01	0.00000E+00	0.0000	7.06103E-14
8.2085E-01	0.00000E+00	0.0000	6.73938E-14
8.6294E-01	0.00000E+00	0.0000	6.13927E-14
9.0718E-01	0.00000E+00	0.0000	5.47065E-14
9.6164E-01	0.00000E+00	0.0000	4.98034E-14
1.0026E+00	0.00000E+00	0.0000	2.84913E-14
1.1080E+00	0.00000E+00	0.0000	9.24000E-14
1.1648E+00	0.00000E+00	0.0000	6.92554E-14
1.2246E+00	0.00000E+00	0.0000	7.68246E-14
1.2873E+00	0.00000E+00	0.0000	7.61766E-14
1.3534E+00	0.00000E+00	0.0000	5.90068E-14
1.4227E+00	0.00000E+00	0.0000	8.41823E-14
1.4957E+00	0.00000E+00	0.0000	8.74303E-14
1.5724E+00	0.00000E+00	0.0000	8.33994E-14
1.6530E+00	0.00000E+00	0.0000	7.15585E-14
1.7377E+00	0.00000E+00	0.0000	8.95265E-14
1.8268E+00	0.00000E+00	0.0000	1.02699E-13
1.9205E+00	0.00000E+00	0.0000	7.10284E-14
2.0190E+00	0.00000E+00	0.0000	8.58058E-14
2.1225E+00	0.00000E+00	0.0000	1.06886E-13
2.2313E+00	0.00000E+00	0.0000	1.29512E-13
2.3069E+00	0.00000E+00	0.0000	1.20015E-13
2.3457E+00	0.00000E+00	0.0000	8.92381E-14
2.3653E+00	0.00000E+00	0.0000	4.97849E-14
2.3852E+00	0.00000E+00	0.0000	3.39496E-14
2.4660E+00	0.00000E+00	0.0000	1.07604E-13
2.5924E+00	0.00000E+00	0.0000	1.07651E-13
2.7253E+00	0.00000E+00	0.0000	1.07556E-13
2.8650E+00	0.00000E+00	0.0000	9.25937E-14
3.0119E+00	0.00000E+00	0.0000	8.72837E-14
3.1664E+00	0.00000E+00	0.0000	7.63306E-14
3.3287E+00	0.00000E+00	0.0000	5.49267E-14
3.6788E+00	0.00000E+00	0.0000	9.52969E-14
4.0657E+00	0.00000E+00	0.0000	1.12844E-13
4.4933E+00	0.00000E+00	0.0000	1.31916E-13
4.7237E+00	0.00000E+00	0.0000	6.84843E-14
4.9659E+00	0.00000E+00	0.0000	7.01860E-14
5.2205E+00	0.00000E+00	0.0000	6.11073E-14
5.4881E+00	0.00000E+00	0.0000	7.63434E-14
5.7695E+00	0.00000E+00	0.0000	4.85169E-14
6.0653E+00	0.00000E+00	0.0000	5.41887E-14
6.3763E+00	0.00000E+00	0.0000	6.82147E-14
6.5924E+00	0.00000E+00	0.0000	4.80000E-14
6.7032E+00	0.00000E+00	0.0000	1.75976E-14
7.0469E+00	0.00000E+00	0.0000	4.42485E-14
7.4082E+00	0.00000E+00	0.0000	3.20668E-14
7.7880E+00	0.00000E+00	0.0000	3.21142E-14
8.1873E+00	0.00000E+00	0.0000	3.21696E-14
8.6071E+00	0.00000E+00	0.0000	2.83227E-14
9.0484E+00	0.00000E+00	0.0000	3.19440E-14
9.5123E+00	0.00000E+00	0.0000	3.59793E-14
1.0000E+01	0.00000E+00	0.0000	3.01604E-14
1.0513E+01	0.00000E+00	0.0000	2.68582E-14
1.1052E+01	0.00000E+00	0.0000	3.11221E-14
1.1618E+01	0.00000E+00	0.0000	1.89707E-14
1.2214E+01	0.00000E+00	0.0000	2.02605E-14
1.2523E+01	0.00000E+00	0.0000	1.29886E-14
1.2840E+01	0.00000E+00	0.0000	1.38341E-14
1.3499E+01	0.00000E+00	0.0000	2.81706E-14
1.3840E+01	0.00000E+00	0.0000	1.74206E-14
1.4191E+01	0.00000E+00	0.0000	1.96044E-14
1.4550E+01	0.00000E+00	0.0000	2.11799E-14
1.4918E+01	0.00000E+00	0.0000	2.42620E-14
1.5683E+01	0.00000E+00	0.0000	5.84903E-14
1.6487E+01	0.00000E+00	0.0000	8.31881E-14
1.6905E+01	0.00000E+00	0.0000	5.62244E-14
1.7333E+01	0.00000E+00	0.0000	4.88567E-14
1.9640E+01	0.00000E+00	0.0000	1.15708E-13
Total	3.41027E-11	0.3416	3.73010E-11

†F4 tally

3. **Activation Calculation**

For an activation calculation, the FISPACT code [8] and activation script [9] are used. Through the activation script, FISPACT works with MCNPX and not MCNP5. Due to this reason, we generate a template data file for FISPACT by running MCNPX with same input as MCNP5 but small number of particles.

The generated template file is used for FISPACT code by replacing neutron spectrum part to those from MCNP5 and AETIUS shown in Fig. 9.

The overall calculation flow for the activation calculation is shown in Fig. 10.

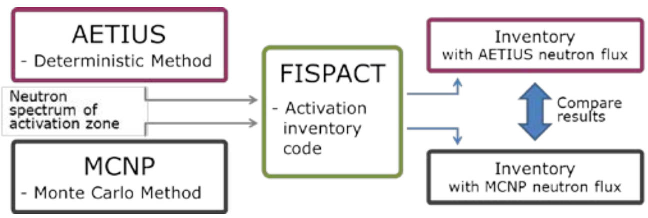

Fig. 10. The overall calculation flow for the activation calculation.

The neutron spectra in Fig. 9 are calculated for one-source-particle and those are used in FISPACT code as basic data. The strength of neutron source is 1×10^{10} neutrons/sec and irradiation time is 2,000 hours. More parameters for activation calculation are listed in Table III.

After 2,000 hours irradiation, we checked the amount of produced nuclides and their activities on the activation zone. In Table IV, the results are listed. More nuclides are produced and activated with spectrum of AETIUS. However, with spectrum of MCNP5, we could not get data for them.

Table III. Parameters for activation calculations

	MCNP5	AETIUS
Irradiation time	2,000 hours	
Strength of neutron source	1×10^{10} neutrons/sec	
Neutron spectrum	Spectrum from MCNP5 in Fig. 9.	Spectrum from AETIUS in Fig. 9.
Activation code	FISPACT	

Table IV. The amount of produced nuclides and their activities in the activation zone

Nuclides	MCNP5 Production (g)	MCNP5 Activity (Bq)	AETIUS Production (g)	AETIUS Activity (Bq)
V-49	n/a	n/a	6.530E-22	1.953E-07
V-50	5.730E-20	1.084E-22	5.994E-20	1.134E-22
Cr-50 >	6.522E-02	9.596E-05	6.522E-02	9.596E-05
Cr-51	8.170E-19	2.797E-03	8.735E-19	2.990E-03
Mn-53	n/a	n/a	4.187E-21	2.843E-13
Mn-54	n/a	n/a	1.539E-20	4.417E-06
Fe-55	1.338E-18	1.178E-04	1.518E-18	1.337E-04
Fe-59	1.901E-20	3.501E-05	2.031E-20	3.741E-05
Co-57	n/a	n/a	1.260E-20	3.933E-06
Co-58	5.196E-20	6.115E-05	4.297E-20	5.057E-05
Co-60	n/a	n/a	1.333E-21	5.581E-08
Ni-58 >	5.109E-01	1.666E-07	5.109E-01	1.666E-07
Ni-59	4.401E-18	1.300E-08	4.660E-18	1.376E-08
Ni-63	7.209E-19	1.506E-06	7.626E-19	1.593E-06

Volume of small activation zone : 1cm^3
> : nuclides that originally existed in material composition but activated.
n/a : not calculated.

In Fig. 11, we compared two decay gamma spectra with AETIUS and MCNP5 neutron spectra. Decay gamma spectrum with AETIUS is greater than that with MCNP5. This is because more nuclides are produced and activated compared to the MCNP5 case.

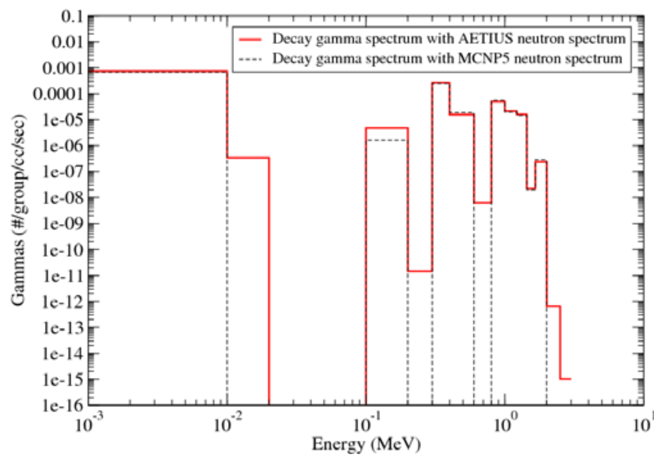

Fig. 11. Two decay gamma spectra with AETIUS and MCNP5 neutron spectra.

III. RESULTS

In this paper, numerical results of an activation calculation in a deep penetration problem with a small detection volume are compared.

The averaged total neutron fluxes in the detection and activation zones show similar results. However, MCNP5 could not provide reliable neutron spectrum in the activation zone. These differences in the neutron spectra cause the different amount of produced nuclides and their activities in the activation zone.

IV. CONCLUSIONS

A brief overview of in-house code, AETIUS, and numerical results from both AETIUS and MCNP5 for an activation calculation in a deep penetration problem with a small detection volume are provided in this paper.

An accurate neutron spectrum is indispensable to have a good shutdown dose or activation calculations. To get a detail neutron spectrum, we increase number of energy groups such that the size of the energy bin is getting smaller and smaller. However, the smaller the size of the energy bin, the larger the relative error in the MCNP tally.

As we can see in this paper, we could get meaningful results on the activation calculation in a deep penetration problem.

Deterministic code, such as AETIUS, is powerful in this kind of problem since it can provide neutron spectrum without any statistics.

Monte Carlo code, such as MCNP, is also useful. However, in this problem, it is not easy to have a good neutron spectrum with reliable relative error since statistic problem always tags along.

REFERENCES

1. X-5 Monte Carlo Team, "MCNP - A General Monte Carlo N-Particle Transport Code, Version 5, Volume II: User's Guide," LA-CP-03-0245, Los Alamos National Laboratory (2008).
2. T.A. Wareing, J.M. McGhee, J.E. Morel, and S.D. Pautz, "Discontinuous Finite Element S_N Methods on Three-Dimensional Unstructured Grids," *Nucl. Sci. Eng.*, 138, 256-268 (2001).
3. C. Geuzaine, J.-F. Remacle, "Gmsh: a three-dimensional finite element mesh generator with built-in pre- and post-processing facilities," *Int. J. Numer. Meth. Eng*. 79 (11) 1309-1331 (2009).
4. J.W. Kim, C.W. Lee, Y. Lee, D. Lee, and S. Cho, "Preliminary study on applying discrete ordinates code supporting unstructured tetrahedral mesh to the 40-degree toroidal segment ITER model," *Fusion Science and Technology*, 68, 652-656 (2015).
5. Barbara Chapman et al., Using OpenMP, The MIT Press, Cambridge, Massachusetts, London, England (2008).
6. S.G. Hong, "Two Subcell Balance Methods for Solving the Multigroup Discrete Ordinates Transport Equation with Tetrahedral Meshes," *Nucl. Sci. Eng.*, 173, 101-117 (2013).
7. J.M. McGhee, T.A. Wareing, and D.A. Barnett Jr., "Attila User's Manual," Transpire Inc. (2007).
8. R. A. Forrest, "FISPACT-2007 User Manual," UKAEA FUS 534, EURATOM/UKAEA Fusion Association, Culham Science Centre (2007).
9. Franz X. Gallmeier and Michael Wohlmuther, "Activation Script Version 1.0 User Guide," ORNL/TM-2008/031, Oak Ridge National Laboratory (2008).